CHEMISTRY OF MATERIALS

ARTICLE

pubs.acs.org/cm

Hybrid, Silica-Coated, Janus-Like Plasmonic-Magnetic Nanoparticles

Georgios A. Sotiriou,[†] Ann M. Hirt,[‡] Pierre-Yves Lozach,[§] Alexandra Teleki,[†,⊥] Frank Krumeich,[†] and Sotiris E. Pratsinis*[,†]

[†]Particle Technology Laboratory, Institute of Process Engineering, Department of Mechanical and Process Engineering, [‡]Institute of Geophysics, Department of Earth Sciences, and [§]Institute of Biochemistry, Department of Biology, ETH Zurich, Sonneggstrasse 3, 8092 Zurich, Switzerland

ABSTRACT: Hybrid plasmonic-magnetic nanoparticles possess properties that are attractive in bioimaging, targeted drug delivery, in vivo diagnosis, and therapy. The stability and toxicity, however, of such nanoparticles challenge their safe use today. Here, biocompatible, SiO_2-coated, Janus-like Ag/Fe_2O_3 nanoparticles are prepared by one-step, scalable flame aerosol technology. A nanothin SiO_2 shell around these multifunctional nanoparticles leaves intact their morphology and magnetic and plasmonic properties but minimizes the release of toxic Ag^+ ions from the nanosilver surface and its direct contact with live cells. Furthermore, this silica shell hinders flocculation and allows for easy dispersion of such nanoparticles in aqueous and biological buffer (PBS) solutions without any extra functionalization step. As a result, these hybrid particles exhibited no cytotoxicity during bioimaging and remained stable in suspension with no signs of agglomeration and sedimentation or settling. Their performance as biomarkers was explored by selectively binding them with live tagged Raji and HeLa cells enabling their detection under dark-field illumination. Therefore, these SiO_2-coated Ag/Fe_2O_3 nanoparticles do not exhibit the limiting physical properties of each individual component but retain their desired functionalities facilitating thus, the safe use of such hybrid nanoparticles in bioapplications.

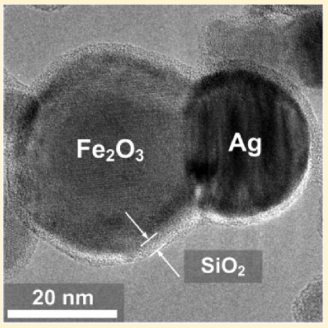

KEYWORDS: silver, iron oxide, silicon dioxide, cancer cell detection, heterodimer

INTRODUCTION

Plasmonic (Au or Ag) nanoparticles are superior markers for cell monitoring in bioimaging, diagnosis and therapy.[1] Such nanoparticles can be readily detected and traced by optical techniques such as light scattering,[2] dark-field illumination,[3] two-photon fluorescence imaging,[4] and photon illumination confocal microscopy.[5] Alternatives to plasmonic nanoparticles for bioimaging are the commonly used fluorescent organic dyes and semiconducting nanoparticles.[6] The former, however, exhibit the so-called photobleaching and degrade during bioimaging.[7] The latter, on the other hand, may exhibit optical blinking,[8] while concerns arise for their toxicity as most contain cadmium or lead.[6] Even though plasmonic nanoparticles also induce toxicity,[9] they are functionally advantageous over fluorescent organic dyes and semiconducting nanoparticles because they have superior photostability[10] and can be used also as photothermal therapeutic agents (e.g., tumor treatment),[5] offering an extra functionality in bioapplications.

When plasmonic nanoparticles are combined with another material, e.g., a magnetic component, multifunctional nanostructured materials[1] are created, that can be detected and guided by multiple imaging and control[11] techniques. Magnetic resonance imaging (MRI) is an example of a traditional technique, with which magnetic particles can be used as contrast agents[12] and for targeted drug delivery by directing them to organs, tissues or tumors using an external magnetic field or for magnetically assisted cell sorting and separation.[11] Furthermore, a SiO_2 film on the surface of such magnetic nanoparticles facilitates their surface biofunctionalization and minimizes their magnetic interactions[13] and flocculation[14] or agglomeration.

Composite plasmonic-magnetic nanostructures are typically made by multistep wet methods. Depending on synthesis route, core/shell[15] or heterodimer (Janus-like)[4] plasmonic-magnetic materials are formed. These "as-prepared" nanoparticles are often hydrophobic requiring a surface modification to stably suspend[4] them in aqueous solutions. Typically, the magnetic material is iron oxide (γ-Fe_2O_3 or Fe_3O_4) for its high spontaneous magnetization[11] in a superparamagnetic state. Live macrophage cells bound on labeled Ag/Fe_3O_4 nanoparticles have been imaged and manipulated[4] by an external magnetic field.

There are limitations, however, that hinder the use of such materials in bioapplications. First and foremost, their toxicity needs to be addressed before they can be employed.[16] Even though Ag has the lowest optical plasmonic losses in the UV—visible spectrum,[17] the more expensive Au nanoparticles are preferred for bioimaging because of their lower cytotoxicity.[9] The release of toxic Ag^+ ions[18] when Ag nanoparticles are dispersed in aqueous solutions blocks their safe use[19] in bioapplications. By coating Ag nanoparticles, however, with a nanothin shell, this toxicity can be eliminated while their surface biofunctionalization can be enhanced by hindering also their flocculation[14] that poses another limitation in the use of plasmonic-magnetic

Received: February 8, 2011
Revised: February 23, 2011
Published: March 09, 2011

dx.doi.org/10.1021/cm200399t | *Chem. Mater.* 2011, 23, 1985–1992

nanomaterials[11,20] when dispersed in aqueous solutions. Overcoming these particle−particle interactions including magnetic ones requires typically additional surface modification of these particles.[1]

Here, one-step synthesis of hybrid, silica-coated, plasmonic-magnetic nanomaterials is explored by scalable[21] flame aerosol technology. The morphology of these composite nanoparticles and the influence of their SiO_2 shell on the release of Ag^+ ions (Ag leaching) is investigated along with their cytotoxicity against HeLa cells and biocompatibility. The magnetic hysteresis of these nanoparticles is examined and the effect of SiO_2-coating on their stability in aqueous and phosphate buffer saline (PBS) solutions is explored. The plasmonic properties of these hybrid nanoparticles are investigated and their magnetic guiding is demonstrated. Finally, the feasibility of these multifunctional materials in bioimaging is studied by selectively labeling live Raji and HeLa cells and monitoring them under dark-field illumination.

EXPERIMENTAL SECTION

Hybrid SiO_2-Coated Ag/Fe_2O_3 Nanoparticle Synthesis. Silica-coated Ag/Fe_2O_3 particles were made in one-step with an enclosed flame aerosol reactor, described in detail elsewhere.[14] In brief, the composite core Ag/Fe_2O_3 nanoparticles were made by flame spray pyrolysis (FSP) of precursor solutions containing iron(III) acetylacetonate (Sigma Aldrich, purity ≥97%) and silver acetate (Sigma Aldrich, purity ≥99%) dissolved in 2-ethylhexanoic acid and acetonitrile (both Sigma Aldrich, purity ≥97%, volume ratio 1:1, stirring 100 °C for 30 min). The precursor solutions were fed at 5 mL/min to the FSP reactor and dispersed by 5 L/min O_2 (all gases Pan Gas, purity >99%) forming a spray (pressure drop =1.5 bar at the nozzle tip) that was ignited by a ring-shaped, premixed methane/oxygen flame (1.5/3.2 L/min) and sheathed by 40 L/min O_2. The Fe precursor concentration was kept constant at 0.5 M, while corresponding amounts of silver acetate were added to reach the nominal Ag wt%, which was defined as $x = m_{Ag}/(m_{Ag} + m_{Fe2O3})$, and labeled as $x Ag/Fe_2O_3$.

The freshly formed composite $x Ag/Fe_2O_3$ particles were coated in-flight by swirl injection of hexamethyldisiloxane (HMDSO, Sigma Aldrich, purity ≥99%) vapor with 15 L/min nitrogen (PanGas, purity > 99.9%) at room temperature through a metallic ring with 16 equidistant openings. The ring was placed on top of a 20 cm long quartz glass tube followed by another 30 cm long such tube. The HMDSO vapor was supplied by bubbling nitrogen through approximately 350 mL liquid HMDSO in a 500 mL glass flask. The SiO_2 amount was kept constant in the product particles and was calculated at saturation conditions[22] (bubbler temperature 10 °C and 0.5 L/min N_2) corresponding to 23 wt % for pure Fe_2O_3 core particles[13] (SiO_2 wt% = $m_{SiO2}/(m_{SiO2} + m_{Fe2O3})$). Silica-coated pure core Ag or Fe_2O_3 particles were made at identical conditions in the absence, however, of the corresponding precursor (Fe or Ag precursor, respectively).

Particle Characterization. High-resolution transmission electron microscopy (HRTEM) and scanning transmission electron microscopy (STEM) was performed on a Tecnai F30 (FEI; field emission gun, operated at 300 kV). The STEM images were recorded with a high-angle annular dark field (HAADF) detector revealing the Ag particles with bright Z contrast. Product particles were dispersed in ethanol and deposited onto a perforated carbon foil supported on a copper grid. X-ray diffraction (*XRD*) patterns were obtained[13,14] with a Bruker AXS D8 Advance spectrometer (Cu Kα, 40 kV, 40 mA). The crystallite size of silver and iron oxide was determined using the TOPAS 3 software and fitting only the main diffraction peaks.

The release of Ag^+ ions was measured by monitoring the Ag^+ ion concentration of aqueous suspensions containing the composite particles.[23] Particles were dispersed by ultrasonication (Sonics vibracell, 5 min at 75% amplitude with a pulse configuration on/off of 0.2s/0.2s) in deionized water (Milli-Q) and their Ag^+ ion concentration was monitored with an ion selective electrode and an ion meter (Metrohm, 867 module).[18] The measurements were calibrated using silver containing aqueous solution (silver standard, Aldrich) with a calibration slope of 59.3 mV/log [Ag^+]. Diffusive gradients in thin film (DGT) measurements were performed and the Ag concentration was measured with an ICP-MS.[18] The optical properties of the composite particles were monitored with UV/vis spectroscopy (Cary Varian 500) of their aqueous suspensions. Particles were dispersed in deionized water and in phosphate PBS solution by ultrasonication (Sonics vibra cell, 5 min, power 50%, pulse on/off 0.2 s/0.2 s). Size distributions of particles in aqueous and PBS solutions and ζ-potential measurements of aqueous suspensions[24] were obtained by dynamic light scattering (DLS, Zetasizer, Malvern Instruments). Magnetic measurements were made on a Princeton Measurements Corporation vibrating sample magnetometer (VSM).

Biocompatibility of the Hybrid Biomarkers. The cytotoxicity of uncoated and SiO_2-coated $35Ag/Fe_2O_3$ nanoparticles was investigated with the human cell line HeLa. The cell viability was monitored by using the LIVE/DEAD fixable dead cell stain kit (Invitrogen) and flow cytometry (~5000 cells counted).[25] Suspensions of nanoparticles in PBS were prepared by ultrasonication as above and added on HeLa cells (2×10^5 cells at a volume ratio of 1:1). The following three incubation conditions were examined: with composite Ag/Fe_2O_3 particle concentration of 5 mg/L (Ag concentration of 1.45 mg/L) (i) at 4 °C for 1 h (identical to the conditions during particle binding with cells for bioimaging) and at Ag concentrations of 5, 2.5, 1.25, and 0.625 mg/L incubated at 37 °C for (ii) 1 and (iii) 24 h. As a negative control to assess viability, pure PBS was added instead of the particle suspension. Staurosporin (20 μM, Sigma) was used as a positive control. This drug induces strong cytotoxicity and consequently apoptosis, leading to cell death. Error bars correspond to the standard deviation of three measurements.

Bioimaging. For bioimaging, 5 mg/L SiO_2-coated $35Ag/Fe_2O_3$ nanoparticles were dispersed by ultrasonication as above in sterile PBS. Purified mouse monoclonal antibody against hDC-SIGN (MAB1621, R&D Systems) was reconstituted in water with a concentration 1 mg/mL. One-hundred microliters of this antibody-containing solution were added in 5 mL of the particle suspension for surface biofunctionalization. After its incubation for 1 h at room temperature, the biofunctionalized particles were washed with PBS three times. HeLa and Raji cells expressing or not the protein hDC-SIGN were washed three times with PBS. The biofunctionalized particles were added to cells (2×10^5 and 5×10^5 cells for HeLa and Raji cells, respectively) in a 1:1 ratio (v/v) reaching a final volume of 2 mL and then incubated for 1 h at 4 °C. As controls, cells which do not express hDC-SIGN were incubated[26] at 4 °C in the presence or absence of biofunctionalized particles. The optical detection was performed with a microscope equipped with a dark-field condenser (Olympus MM) and a black-and-white CCD camera. The biofunctionalization was verified by monitoring the shift of the plasmon absorption band of the nanosilver[14] with a UV/vis spectrometer (Varian Cary 500).

RESULTS AND DISCUSSION

Morphology. Uncoated and SiO_2-coated $x Ag/Fe_2O_3$ nanoparticles were made with varying Ag-content x (wt %). Figure 1a shows an STEM image of uncoated $50Ag/Fe_2O_3$. There are Ag nanoparticles (bright spots) attached onto Fe_2O_3 particles (gray) forming dumbbell- or Janus-like particles. Figure 1b shows a TEM image of SiO_2-coated $10Ag/Fe_2O_3$ nanoparticles where Ag particles (dark spots) are attached on the Fe_2O_3 particles (gray)

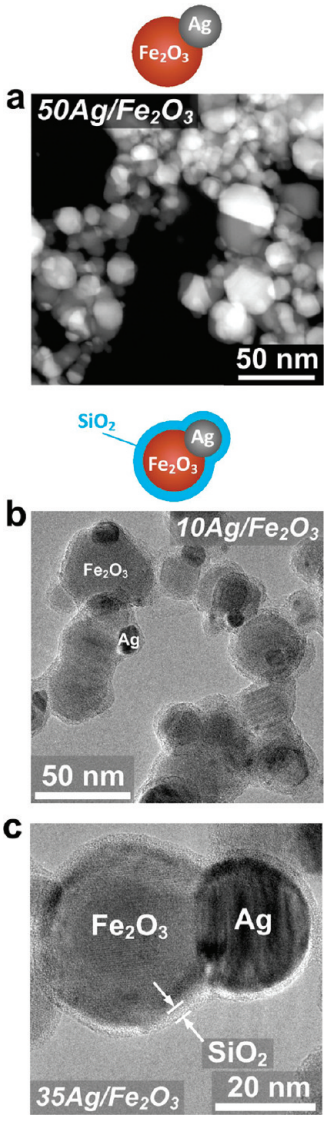

Figure 1. A HAADF-STEM (Z contrast) image of (a) the uncoated $50Ag/Fe_2O_3$ sample and TEM images of (b) the SiO_2-coated $10Ag/Fe_2O_3$ and (c) the SiO_2-coated $35Ag/Fe_2O_3$ sample. Above the images, a schematic drawing of the uncoated and SiO_2-coated particles is presented, for which the red, gray and blue colors correspond to iron oxide, silver, and silica particles, respectively.

as in Figure 1a, but there is an amorphous (light gray) SiO_2 shell or film encapsulating the core Ag/Fe_2O_3 particles. Figure 1c shows this more clearly with an image of a SiO_2-coated $35Ag/Fe_2O_3$ nanoparticle at higher magnification. The iron oxide and the silver particles are completely coated by a smooth, amorphous SiO_2 shell or film of a couple nm thickness.[13] All STEM and TEM images indicate that there is no significant trace of individual or separate Ag or Fe_2O_3 particles, a prerequisite for their bioapplication. The average crystal size of the γ-Fe_2O_3 is approximately 15 nm and independent of the presence of Ag or SiO_2, even though there is a small presence of α-Fe_2O_3 within the samples.[13] The α-Fe_2O_3 content was slightly increased at Ag-content x = 50 wt %. This could be attributed to the higher combustion enthalpy of the employed precursor solutions for the largest Ag-content, and thus higher temperatures within the enclosed flame aerosol reactor.[13] The average Ag crystal size

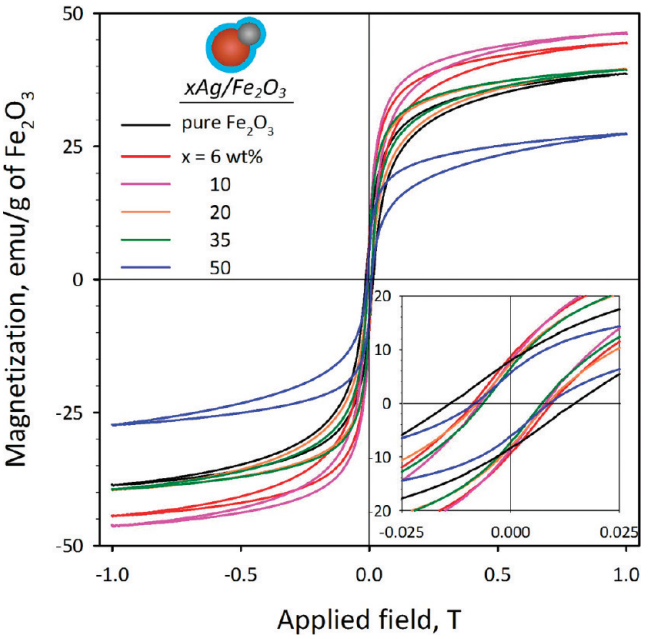

Figure 2. Magnetization curves of the SiO_2-coated xAg/Fe_2O_3 samples. The magnetization values have been normalized for an equal mass of Fe_2O_3. The inset shows a magnification at low magnetic fields highlighting the coercivity and remanence of the particles. The hybrid SiO_2-coated Ag/Fe_2O_3 nanoparticles exhibit a near superparamagnetic behavior.

increases with increasing Ag-content[23] (from ~10 nm for the $20Ag/Fe_2O_3$ to ~20 nm for the $50Ag/Fe_2O_3$) and was also rather independent from the presence of the SiO_2 shell.

Magnetic and Plasmonic performance. Figure 2a shows the magnetization of all SiO_2-coated particles normalized to their Fe_2O_3 mass at various Ag-contents x at room temperature. All particles show some hysteresis, which indicates that are magnetically blocked during the measurement. The coercive force, however, is very low (inset of Figure 2a) while the SiO_2-coating does not influence[13] their magnetic properties. The highest magnetization (M_s = 39.4−46.1 emu/g) of the lower Ag-content particles (x = 6−35 wt %) is similar to pure Fe_2O_3 core (38.4 emu/g). These M_s values are lower than that of bulk γ-Fe_2O_3 (63.6 emu/g),[27] as smaller crystallites[13] are employed here that contain[27] α-Fe_2O_3.

Figure 3a shows the UV/vis absorbance of the SiO_2-coated hybrid particles for x = 10 (purple), 20 (yellow) 35 (green) and 50 wt % (blue) here in aqueous suspensions before (B = 0, solid lines) and after application (B > 0, broken lines) of an external magnetic field by a permanent Ni−Cu−Ni magnet (inset). At B = 0 for the $10Ag/Fe_2O_3$ (purple line) the Ag-content is rather low and the Ag-metal plasmon absorption band is not distinguishable as the spectrum is dominated by the Fe_2O_3 absorption. However, for an increasing Ag-content x > 10 wt % the Ag plasmon band clearly emerges[20] at ~400 nm. This indicates that the optical properties of Ag nanoparticles are not influenced[28] by the presence of Fe_2O_3 nor SiO_2. At B > 0, however, all absorption spectra (from Fe_2O_3 and Ag) disappeared completely and the suspension is transparent, since all particles have been attracted to the cuvette bottom (Figure 3a, inset) by the magnet. This further verifies that there are no individual Ag nanoparticles present in the as-prepared sample, but only composite Ag/Fe_2O_3

dx.doi.org/10.1021/cm200399t |*Chem. Mater.* 2011, 23, 1985–1992

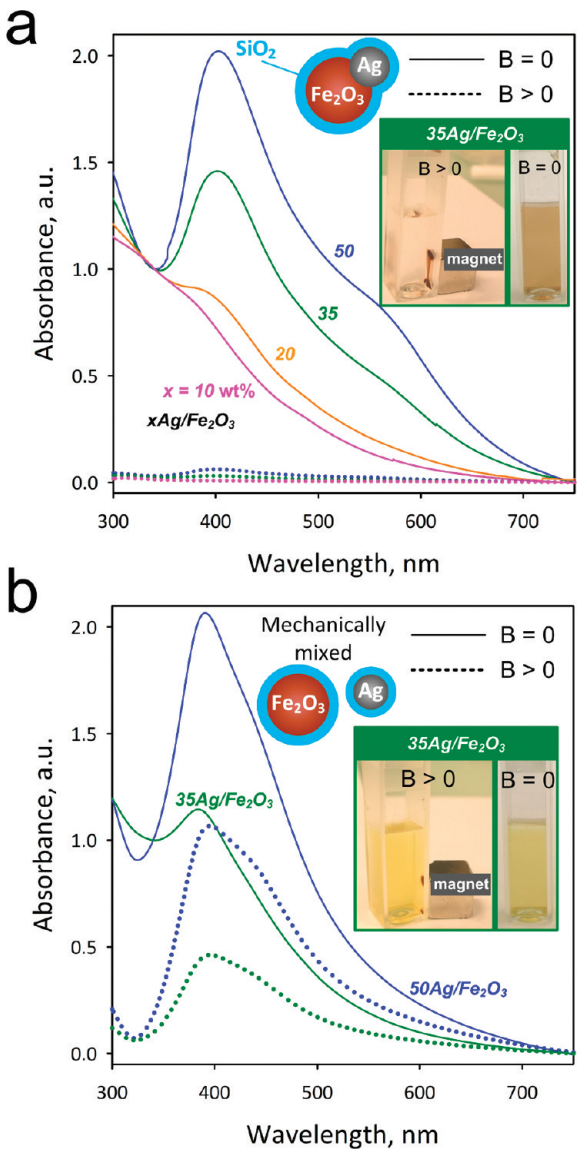

Figure 3. (a) Optical absorption spectra of the SiO_2-coated xAg/Fe_2O_3 before (solid lines) and after their removal with the application of an external magnetic field (broken lines). In the inset, a photograph of the aqueous suspensions before and after the magnetic field of the SiO_2-coated 35Ag/Fe_2O_3 sample. (b) Optical absorption spectra of mechanically mixed SiO_2-coated Ag and Fe_2O_3 nanoparticles, before (solid lines) and after (broken lines) the application of an external magnetic field.

(Figure 1) that were moved by a magnetic field. Therefore, these hybrid nanoparticles could be employed in bioapplications where both magnetic manipulation and optical monitoring are desired.

As a control experiment, separate pure nanosilver[14] and iron oxide[13] nanoparticles, both SiO_2-coated were made by FSP and mechanically mixed (for Ag contents x = 35 and 50 wt %) in water as in Figure 3a. These suspensions also exhibit the plasmon absorption band of Ag nanoparticles (Figure 3b). However, after applying an external magnetic field ($B > 0$), the plasmon band is still distinguishable at 400 nm (broken lines) as only the SiO_2-coated Fe_2O_3 particles were attracted to the cuvette bottom by the magnet. The reduced intensity of the plasmon absorption band at $B > 0$ is attributed to the absence of absorption by the Fe_2O_3 particles. The SiO_2-coated pure Ag particles, however, remained dispersed in solution (Figure 3b, inset, $B > 0$) exhibiting the characteristic yellowish color that is attributed to that nanosilver size[14] and concentration.

Stability in Aqueous Suspensions and Buffer Solutions. When multifunctional (hybrid) nanoparticles are employed in bioimaging, they have to be stable in solution. Figure 4 shows the hydrodynamic size distributions of the SiO_2-coated (a) and uncoated (b) 35Ag/Fe_2O_3 particles in water (solid lines) and in PBS (broken lines) immediately after their dispersion (t = 0 h). The SiO_2-coated particles (a) have quite a low degree of agglomeration in both water and PBS (d_p = 50−500 nm). The uncoated samples (b), however, have a bimodal distribution and much larger agglomerate diameters (500−7000 nm), reaching the limit of the particle size measurement. That is attributed to the absence of SiO_2 which acts as an antiflocculation agent,[14] as the SiO_2-coated particles are stable when dispersed in water and PBS (Figure 4c). In contrast, the formation of the larger agglomerates of uncoated particles results in their sedimentation within both aqueous and PBS suspensions (after 2 h) as seen in Figure 4d.

This stability is especially desired for bioapplications otherwise the resulting agglomerates (flocs) would be similarly sized to the target biological systems (e.g., Raji or HeLa cells) prohibiting their use for cell imaging. Additionally, these silica-coated particles are hydrophilic[22] as-prepared and therefore readily dispersible without requiring an extra functionalization step. The exhibited stability of the SiO_2-coated hybrid nanoparticles is further verified by ζ-potential measurements in water. For all Ag-contents (x = 0−50 wt %) the ζ-potential of the SiO_2-coated particles varies from −42 to −48 mV, in agreement with other SiO_2-coated nanoparticles made by flame[24] or wet chemistry.[29] For the uncoated Ag/Fe_2O_3 particles, the ζ-potential lies from −0.5 to −5.0 mV, also in agreement with those of wet-made Fe_2O_3[30] or Ag[31] nanoparticles.

Biocompatibility of SiO_2-Coated Hybrid Plasmonic-Magnetic Biomarkers. To evaluate the effect of the SiO_2 shell or film on the core Ag/Fe_2O_3 particles on the Ag^+ ion release (leaching), the Ag^+ ion concentration, [Ag^+] (Figure 5a), was monitored in aqueous suspensions of silica-coated and uncoated Ag/Fe_2O_3 by ion selective electrode (ISE, open symbols)[23] and diffusive gradients in thin film (DGT, filled symbols)[18] measurements. Figure 5a shows this [Ag^+] as a function of Ag-content x (in the xAg/Fe_2O_3 particles) for the uncoated (triangles) and SiO_2-coated (circles) particles, for an equal Ag mass concentration of 50 mg/L. The [Ag^+] was attained immediately upon dispersion and was constant over a period of, at least, 24 h.[23] The value obtained when deionized water was measured by ISE are also shown (gray broken line). There was a good agreement between ISE and DGT for the uncoated 35Ag/Fe_2O_3: the silver mass dissolved as silver ions was 7 ± 1.7% by ISE and 8.6 ± 0.5% by DGT. For the SiO_2-coated there was a small difference, the silver dissolved fraction was 2.8 ± 1.4% by ISE, and 5.4 ± 0.5% by DGT.

Uncoated particles release more Ag^+ ions for lower Ag-content xAg/Fe_2O_3 nanoparticles[23] that contain smaller Ag nanoparticles. As the Ag-content x increases, Ag nanoparticles grow bigger releasing less Ag^+ ions[23] from their surface. Silica-coated xAg/Fe_2O_3 release much less [Ag^+] especially for the fine Ag nanoparticles (d_p < 20 nm at x = 6−50 wt %). As the Ag-content x increases, a minimal Ag^+ ion release for x = 50 wt % occurs, which is comparable to the SiO_2-coated Ag/Fe_2O_3 nanoparticles. Nevertheless, the uncoated 50Ag/Fe_2O_3 particles

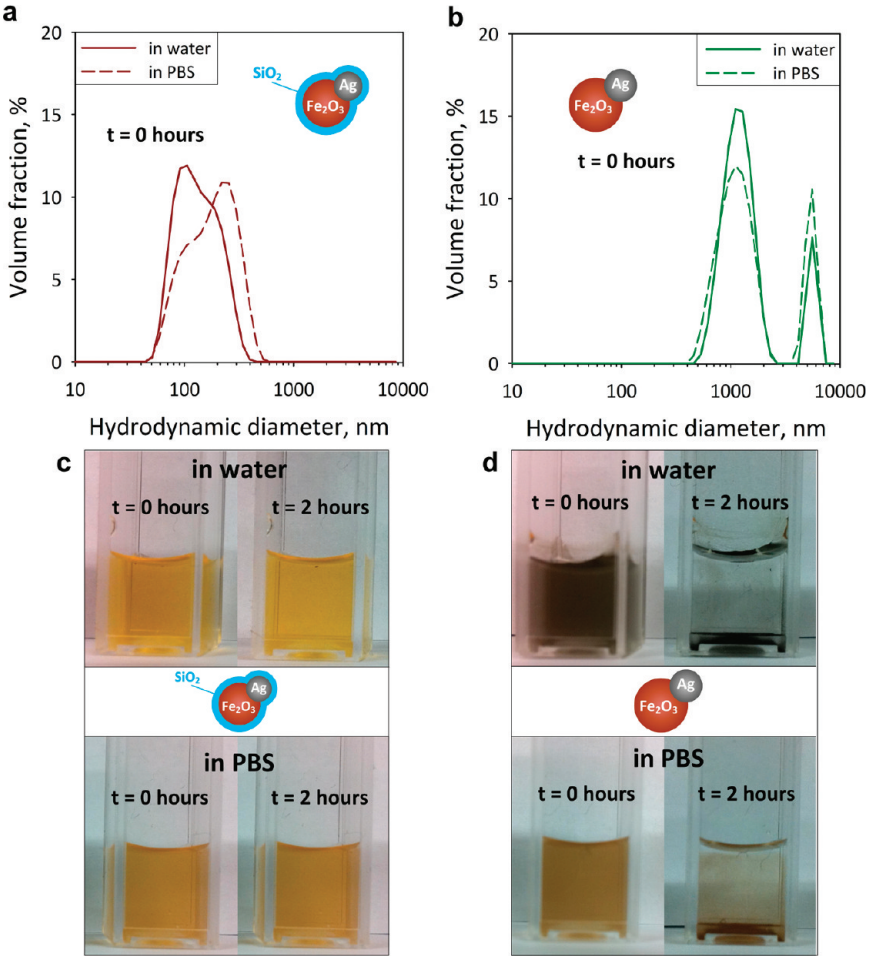

Figure 4. Agglomerate (a) SiO_2-coated and (b) uncoated 35Ag/Fe_2O_3 particle size distributions as determined by dynamic light scattering (hydrodynamic diameter) in water (solid lines) and in phosphate buffer saline (PBS) solution (broken lines) immediately after their dispersion (t = 0 h). Images of dispersion of the (c) SiO_2-coated and (d) uncoated 35Ag/Fe_2O_3 nanoparticles immediately after their dispersion (t = 0 h) and after 2 h in water (top) and PBS (bottom). The hybrid SiO_2-coated Ag/Fe_2O_3 nanoparticles remain stable while the uncoated ones flocculate (agglomerate) and settle after a few hours.

have the lowest magnetization and poor stability in aqueous suspensions (Figure 4d). For the lower Ag content x (6−35 wt %), however, the inert silica shell minimizes nanosilver leaching significantly, but not completely. Few Janus-like particles have been partially coated by incomplete mixing[32,33] of HMDSO vapor with the core Ag/Fe_2O_3 nanoparticles.

To assess the cytotoxicity and biocompatibility of these particles as biomarkers, we incubated them for 24 h at 37 °C with HeLa cells. Figure 5b shows the fraction of dead HeLa cells for different biomarker particle concentrations (5, 2.5, 1.25, and 0.625 mg/L Ag), as well as for the positive and negative controls. In the absence of toxic agents (negative control), there is no significant fraction of apoptotic cells (only the standard, ∼ 10%).[34] The SiO_2-coated hybrid biomarkers did not induce any toxicity for this incubation period (24 h), further indicating their biocompatibility with HeLa cells. The toxicity evaluation of the uncoated plasmonic-magnetic nanoparticles was not possible, as these particles formed large agglomerates and settled quite fast (Figure 4d), thus not giving reliable toxicity results. This emphasizes the limitations of toxicological tests of agglomerated nanoparticles, as their sedimentation inhibits their correct evaluation. It should be noted that for incubation conditions of 1 h at 4 and 37 °C with the SiO_2-coated Ag/Fe_2O_3 nanoparticles, similar results were obtained and no apoptotic cells were detected (not shown).

Bioimaging. The potential of these multifunctional nanoparticles as biomarkers is explored by selectively binding them on tagged living cells. So the surface of SiO_2-coated 35Ag/Fe_2O_3 nanoparticles was labeled (biofunctionalized) with an antibody against the human form of DC-SIGN (hDC-SIGN). Figure 6a shows a shift $\Delta\lambda \approx 10$ nm of the Ag metal normalized plasmon absorption band of these particles after antibody adsorption[14,20] on their surface. The higher refractive index of the antibody over that of PBS causes a red shift[14,20] of the Ag plasmon absorption band. This shift remains even after washing the nanoparticles with PBS, excluding thus the effect of medium change.

Figure 6b shows a dark-field image of Raji cells that do not express hDC-SIGN on their surface (untagged Raji cells) in the absence of labeled particles. The characteristic scattering from the cell membrane as well as from intracellular components can be barely observed.[3] With the exception of very few residual scatterings, probably originating from unwashed labeled particles, identical results were obtained when such cells were incubated with labeled particles (Figure 6c). This suggests that

dx.doi.org/10.1021/cm200399t |*Chem. Mater.* 2011, 23, 1985–1992

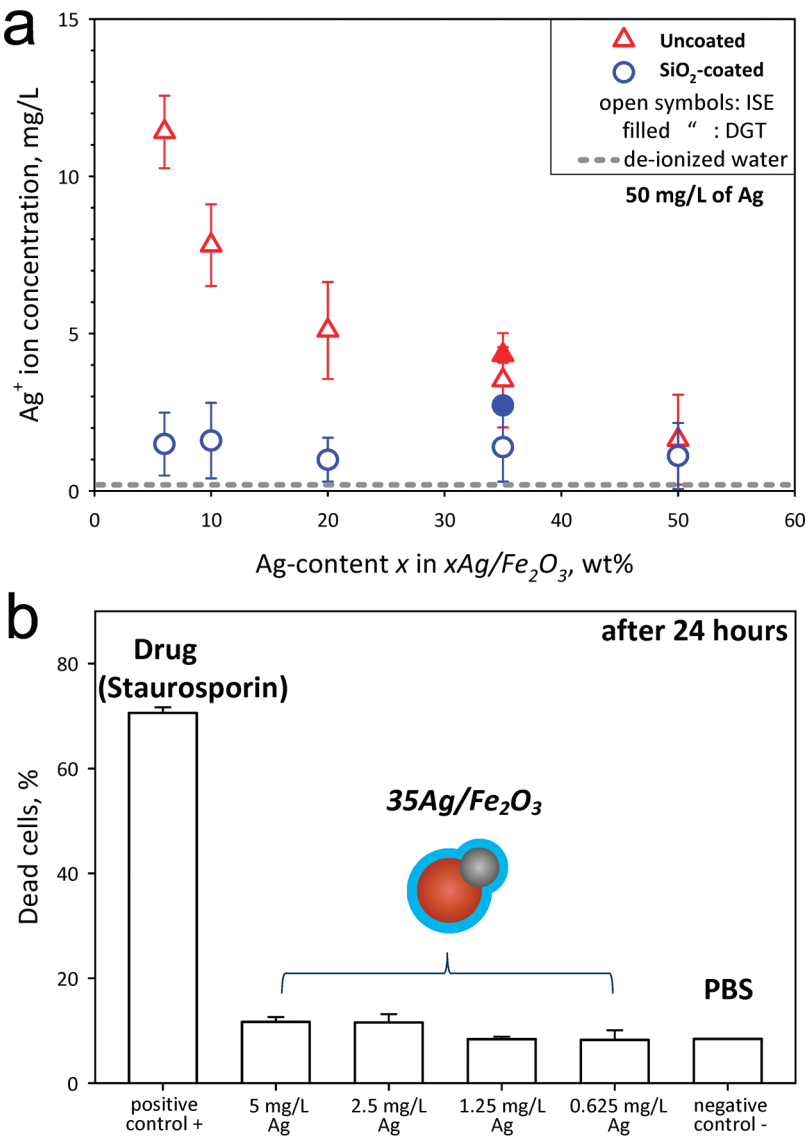

Figure 5. (a) Ag^+ ion concentration of suspensions containing the dispersed uncoated (red triangles) and SiO_2-coated (blue circles) Ag/Fe_2O_3 particles as determined from ISE (open symbols) and DGT (filled symbols). The ISE values of the deionized water are also shown (gray broken line). There is significant release of toxic Ag^+ ions for the uncoated samples, while for the coated ones it is minimized. The error bars correspond to the standard deviation of at least three measurements. (b) The cytotoxicity evaluation of the uncoated and SiO_2-coated $35Ag/Fe_2O_3$ biomarker incubated at 37 °C for 24 h at concentrations 5, 2.5, 1.25, and 0.625 mg/L Ag. The positive (toxic drug inducing apoptosis, Staurosporin) and negative controls are also shown. The error bars correspond to the standard deviation of triplicates.

the SiO_2-coated $35Ag/Fe_2O_3$ particles labeled with the antibody against hDC-SIGN do not unspecifically bind to the cell surface.

In contrast, when Raji cells, that express hDC-SIGN on their surface (tagged cells), are incubated with the labeled particles, it can be seen that the surface of the cells is completely covered by the present hybrid particles (Figure 6d) that strongly scatter light and appear very bright (Ag) under dark-field-illumination.[3] This indicates that by labeling the surface of these nanoparticles with an antibody, they can specifically bind to cells that express the corresponding ligand biomolecule. Additionally, the magnetic manipulation of such cells was possible in the presence of an external magnetic field (permanent magnet, not shown).

These biofunctionalized biomarkers were also used with human HeLa cells that also express the hDC-SIGN. Similarly to the Raji cells, untagged HeLa cells show limited scattering (Figure 6e). When, however, cells that express on their surface the hDC-SIGN are incubated with particles labeled with antibodies against DC-SIGN (Figure 6f), there is a strong scattering originating from the plasmonic silver, and enabling their detailed imaging and fast detection.

CONCLUSIONS

Hybrid, Janus- or dumbbell-like Ag/Fe_2O_3 nanoparticles are made and coated with a nanothin SiO_2 shell or film by one-step, scalable flame aerosol technology. These "as-prepared" nanoparticles were dispersible in aqueous and buffer solutions without any surface treatment. The plasmon absorption band of Ag appeared clearly for an increasing Ag content and size, and the near superparamagnetic Fe_2O_3 component allowed for the

dx.doi.org/10.1021/cm200399t |*Chem. Mater.* 2011, 23, 1985–1992

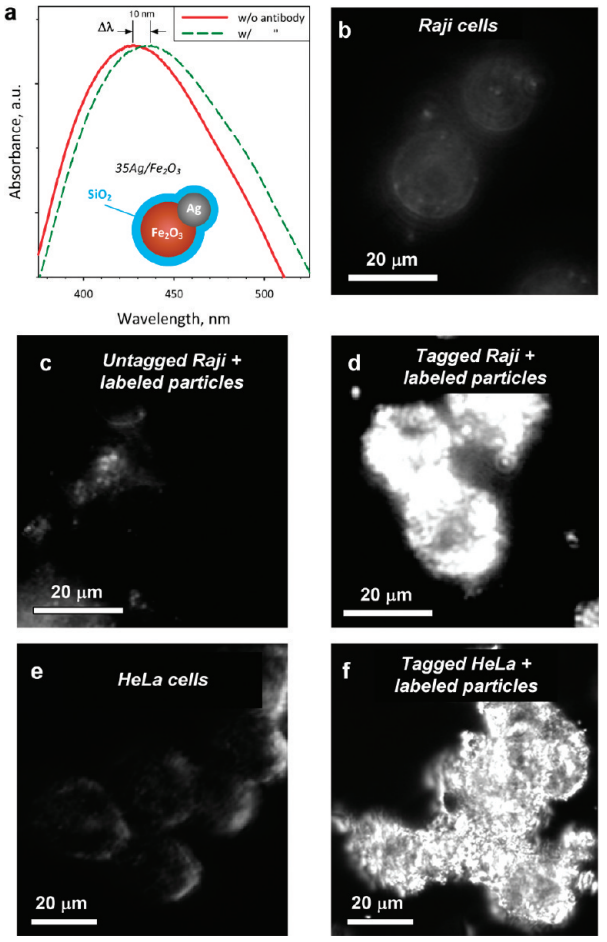

Figure 6. (a) Plasmon absorption band of the SiO_2-coated 35Ag/Fe_2O_3 hybrid plasmonic-magnetic biomarkers before (solid red line) and after (broken green line) their labeling (biofunctionalization) with the antibody. The wavelength shift $\Delta\lambda$ represents the adsorption of the antibody on the surface of the nanoparticles. Dark-field images of the Raji cells that do not express the tag (untagged) (b) without any particles or (c) with labeled particles, and (d) Raji cells that express the tag (tagged) with labeled particles are shown. In contrast to the images of (b, c) parental Raji cells that do not express the tag, (d) the surface of the cells has been completely covered by the particles when the tagged cells were used. Similarly, (e) dark-field images of HeLa cells that express the tag and (f) incubated with the labeled biomarkers show significant differences enabling their readily detection.

magnetic manipulation of the Ag/Fe_2O_3 nanoparticles in aqueous suspensions. The SiO_2 coating reduced drastically the release of Ag^+ ions when nanoparticles were dispersed in aqueous suspensions, essentially "curing" their cytotoxicity and enabling them as biocompatible multifunctional probes for bioimaging. Their agglomeration (flocculation) in aqueous suspensions was minimized by SiO_2 coating, in contrast to uncoated Ag/Fe_2O_3 particles which flocculated and settled within few hours.

The potential of these superior hybrid plasmonic-magnetic nanoparticles as bioprobes was explored by successfully labeling their surface and specifically binding them on the membrane of tagged Raji and HeLa cells. Their detection under dark-field illumination was achieved. The hybrid nanocomposite SiO_2-coated Ag/Fe_2O_3 particles prevented the individual limitations of Fe_2O_3 (poor particle stability in suspensions) and of Ag (toxicity) nanoparticles, while retaining the desired magnetic properties of Fe_2O_3, the inert surface of SiO_2 and the plasmonic optical properties of Ag at the nanoscale.

AUTHOR INFORMATION

Corresponding Author

*E-mail: pratsinis@ptl.mavt.ethz.ch.

Present Addresses

⊥currently at DSM Nutritional Products Ltd., Basel, Switzerland.

ACKNOWLEDGMENT

We thank Dr. Justine Kusch and the light microscopy center (LMC), Dr. Sung Sik Lee (Institute of Biochemistry) for their valuable help with the dark-field microscopy and electron microscopy center (EMEZ) all in ETH Zurich. We thank Dr. Niksa Odzak and Prof. Laura Sigg (EAWAG, Switzerland) for the DGT measurements. Financial support by the Swiss National Science Foundation (200020-126694) and the European Research Council is kindly acknowledged. P.-Y.L. was supported by a Marie Curie Intra European Fellowship within the seventh European Community Framework Programme.

REFERENCES

(1) Zeng, H.; Sun, S. H. *Adv. Funct. Mater.* **2008**, *18*, 391–400.
(2) El-Sayed, I. H.; Huang, X. H.; El-Sayed, M. A. *Nano Lett.* **2005**, *5*, 829–834.
(3) Aaron, J.; Travis, K.; Harrison, N.; Sokolov, K. *Nano Lett.* **2009**, *9*, 3612–3618.
(4) Jiang, J.; Gu, H. W.; Shao, H. L.; Devlin, E.; Papaefthymiou, G. C.; Ying, J. Y. *Adv. Mater.* **2008**, *20*, 4403–4407.
(5) Wang, C. G.; Chen, J.; Talavage, T.; Irudayaraj, J. *Angew. Chem., Int. Ed.* **2009**, *48*, 2759–2763.
(6) Medintz, I. L.; Uyeda, H. T.; Goldman, E. R.; Mattoussi, H. *Nat. Mater.* **2005**, *4*, 435–446.
(7) Das, G. K.; Tan, T. T. Y. *J. Phys. Chem. C* **2008**, *112*, 11211–11217.
(8) Nirmal, M.; Dabbousi, B. O.; Bawendi, M. G.; Macklin, J. J.; Trautman, J. K.; Harris, T. D.; Brus, L. E. *Nature* **1996**, *383*, 802–804.
(9) Singh, S.; D'Britto, V.; Prabhune, A. A.; Ramana, C. V.; Dhawan, A.; Prasad, B. L. V. *New J. Chem.* **2010**, *34*, 294–301.
(10) Lee, K. J.; Nallathamby, P. D.; Browning, L. M.; Osgood, C. J.; Xu, X. H. N. *ACS Nano* **2007**, *1*, 133–143.
(11) Lu, A. H.; Salabas, E. L.; Schuth, F. *Angew. Chem., Int. Ed.* **2007**, *46*, 1222–1244.
(12) Weissleder, R.; Elizondo, G.; Wittenberg, J.; Rabito, C. A.; Bengele, H. H.; Josephson, L. *Radiology* **1990**, *175*, 489–493.
(13) Teleki, A.; Suter, M.; Kidambi, P. R.; Ergeneman, O.; Krumeich, F.; Nelson, B. J.; Pratsinis, S. E. *Chem. Mater.* **2009**, *21*, 2094–2100.
(14) Sotiriou, G. A.; Sannomiya, T.; Teleki, A.; Krumeich, F.; Vörös, J.; Pratsinis, S. E. *Adv. Funct. Mater.* **2010**, *20*, 4250–4257.
(15) Lim, J.; Eggeman, A.; Lanni, F.; Tilton, R. D.; Majetich, S. A. *Adv. Mater.* **2008**, *20*, 1721–1726.
(16) Anker, J. N.; Hall, W. P.; Lyandres, O.; Shah, N. C.; Zhao, J.; Van Duyne, R. P. *Nat. Mater.* **2008**, *7*, 442–453.
(17) Barnes, W. L.; Dereux, A.; Ebbesen, T. W. *Nature* **2003**, *424*, 824–830.
(18) Navarro, E.; Piccapietra, F.; Wagner, B.; Marconi, F.; Kaegi, R.; Odzak, N.; Sigg, L.; Behra, R. *Environ. Sci. Technol.* **2008**, *42*, 8959–8964.
(19) Schrand, A. M.; Braydich-Stolle, L. K.; Schlager, J. J.; Dai, L. M.; Hussain, S. M. *Nanotechnology* **2008**, *19*, 235104–235117.

(20) Willets, K. A.; Van Duyne, R. P. *Annu. Rev. Phys. Chem.* **2007**, *58*, 267–297.
(21) Mueller, R.; Madler, L.; Pratsinis, S. E. *Chem. Eng. Sci.* **2003**, *58*, 1969–1976.
(22) Teleki, A.; Heine, M. C.; Krumeich, F.; Akhtar, M. K.; Pratsinis, S. E. *Langmuir* **2008**, *24*, 12553–12558.
(23) Sotiriou, G. A.; Pratsinis, S. E. *Environ. Sci. Technol.* **2010**, *44*, 5649–5654.
(24) Teleki, A.; Akhtar, M. K.; Pratsinis, S. E. *J. Mater. Chem.* **2008**, *18*, 3547–3555.
(25) Ammar, D. A.; Noecker, R. J.; Kahook, M. Y. *Adv. Ther.* **2010**, *27*, 837–845.
(26) Lozach, P. Y.; Lortat-Jacob, H.; de Lavalette, A. D.; Staropoli, I.; Foung, S.; Amara, A.; Houles, C.; Fieschi, F.; Schwartz, O.; Virelizier, J. L.; Arenzana-Seisdedos, F.; Altmeyer, R. *J. Biol. Chem.* **2003**, *278*, 20358–20366.
(27) Peters, C.; Dekkers, M. J. *Phys. Chem. Earth* **2003**, *28*, 659–667.
(28) Gole, A.; Agarwal, N.; Nagaria, P.; Wyatt, M. D.; Murphy, C. J. *Chem. Commun.* **2008**, 6140–6142.
(29) Zhai, J.; Tao, X.; Pu, Y. A.; Zeng, X. F.; Chen, J. F. *Appl. Surf. Sci.* **2010**, *257*, 393–397.
(30) Kang, Y. S.; Lee, D. K.; Lee, C. S.; Stroeve, P. *J. Phys. Chem. B* **2002**, *106*, 9341–9346.
(31) Tai, C. Y.; Wang, Y. H.; Liu, H. S. *AIChE J.* **2008**, *54*, 445–452.
(32) Teleki, A.; Buesser, B.; Heine, M. C.; Krumeich, F.; Akhtar, M. K.; Pratsinis, S. E. *Ind. Eng. Chem. Res.* **2009**, *48*, 85–92.
(33) Buesser, B.; Pratsinis, S. E. *AIChE J.* **2011**, DOI: 10.1002/aic.12512.
(34) Massich, M. D.; Giljohann, D. A.; Schmucker, A. L.; Patel, P. C.; Mirkin, C. A. *ACS Nano* **2010**, *4*, 5641–5646.